Chemistry Africa (2024) 7:2005–2016
https://doi.org/10.1007/s42250-023-00849-3

ORIGINAL ARTICLE

Antioxidant, Cytotoxicity, and Anti-inflammation Activities of Phenanthroline Adducts of Zn(II) and Ni(II) bis(*N*-alkyl-*N*-phenyldithiocarbamate)

Tanzimjahan A. Saiyed[1,2] · Jerry O. Adeyemi[1,3] · Moganavelli Singh[3] · Damian C. Onwudiwe[4]

Received: 22 May 2023 / Accepted: 27 November 2023 / Published online: 18 January 2024

Abstract

In this study, 4,7-diphenyl-1,10-phenanthroline adducts of Ni(II) and Zn(II) of *N*-methyl or ethyl-*N*-phenyldithiocarbamate were synthesized and the final adducts were represented as **$[Zn(L^1)_2L^3]$, $[Zn(L^2)_2L^3]$, $[Ni(L^1)_2L^3]$, $[Ni(L^2)_2L^3]$** (where L^1 = methyl, L^2 = ethyl, L^3 = bathophenanthroline) and characterized using various spectroscopic techniques and elemental analysis. Both the FT-IR and NMR analysis suggest that all the adducts possessed six coordination geometry by the metal atom centres upon the emergence of a new M-N bond. This was shown by the changes observed in the peaks and chemical shifts of the adducts in comparison to the parent complexes. The cytotoxicity, antioxidant, and anti-inflammatory properties were evaluated using different assays to ascertain their biological properties. In all the assays, no noticeable trend was observed between the adducts of similar ligands and metals. Nevertheless, in the antioxidant assays, a good to moderate activity was observed, especially in the DPPH assay, which gave the best radical scavenging properties. Additionally, the estimated IC_{50} values of 0.011 and 14.76 μM were calculated for the cytotoxicity in the human cervical cancer (HeLa) cell line for both **$[Zn(L^1)_2L^3]$** and **$[Ni(L^2)_2L^3]$** adducts, respectively, in comparison to 5-Flurouracil (17.48 μM). On the other hand, very low cytotoxicity was found for most of the adducts in the embryonic kidney 293 (HEK 293) cell lines, especially for **$[Zn(L^1)_2L^3]$**, demonstrating its superior amongst the other adduct and the standard drug. Moreover, the adducts exhibited good to moderate anti-inflammatory properties compared to diclofenac, a controlled drug. These findings thus suggest that the adducts, particularly **$[Zn(L^1)_2L^3]$,** hold promise as potential anticancer agents and warrant further evaluation through clinical trials.

Keywords Zinc · Nickel · 1,10-phenanthroline · Adducts · Dithiocarbamate · Cytotoxicity · Antioxidant · Anti-inflammatory

✉ Jerry O. Adeyemi
jerryadeyemi1st@gmail.com

✉ Damian C. Onwudiwe
Damian.Onwudiwe@nwu.ac.za

[1] Material Science Innovation and Modelling (MaSIM) Research Focus Area, Faculty of Natural and Agricultural Science, North-West University (Mafikeng Campus), Private Bag X2046, Mmabatho, South Africa

[2] Department of Chemistry, Faculty of Natural and Agricultural, Science, North-West University (Mafikeng Campus), Private Bag X2046, Mmabatho 2735, South Africa

[3] Department of Botany and Plant Biotechnology, Postharvest and Agro-processing Research Centre, University of Johannesburg, Auckland Park, P.O. Box 524, Johannesburg 2006, South Africa

[4] Nano-Gene and Drug Delivery Laboratory, Department of Biochemistry, University of KwaZulu-Natal, Private Bag X54001, Durban 4000, South Africa

1 Introduction

Metal complexes have a vital function in the human biological system. As a result, in recent times, varied pharmaceutical research continues to explore innovative approaches to their application as medicine [1]. They are more suited to targeting specific biological locations due to their vast range of geometries and coordination characteristics [1]. Metal complexes containing central metal atoms or ions, such as zinc, copper, iron, and others, play an important role in a variety of biological processes, including photosynthesis, oxygen transport in the blood, electron transfer to catalysis for structural roles, and enzymatic reactions involving active sites of proteins and enzymes [2]. The shortage of specific metal ions such as zinc, iron, and copper in the human body has been implicated as the cause of many diseases like pernicious anemia, growth retardation, and heart disease in infants, respectively [3]. There is, thus, a continuous need for research in medical bioinorganic chemistry to understand and treat diseases caused by insufficient metal-ion activity at the molecular level [1]. Metal complexes have several oxidation states, and their cationic form has a unique role in the biological system; as a result, metal ions become electron deficient and soluble in bio-fluid [4, 5]. Most biomolecules, including DNA, enzymes, and proteins, are, on the other hand, surrounded by clouds of electrons, which in turn leads to the interaction of metal ions due to their opposing charges [6]. Based on this fundamental principle, a wide range of metallodrugs has been developed, resulting in significant discoveries in inorganic chemistry and improved prospects to employ metal complexes as therapeutic agents. Due to the presence of the metal ion, the complexation of metals with organic ligands has been reported to result in increased biological activities of the organic component of the metal medication [7]. This might be due to the extended retention time of these medications, which permits them to reach the intended targeted sites more efficiently or could be related to the generation of reactive oxygen species (ROS), among other things [7].

Dithiocarbamate complexes are a notable class of metal complexes that have garnered significant attention as potential biological agents due to their diverse chemical properties and therapeutic potential [8]. Their usefulness arises from their unique chemistry, which enables interactions with various biological targets and modulation of critical cellular processes [9]. The dithiocarbamate ligands are known for their coordination properties, forming stable complexes with transition metals [9]. The chelation theory suggests that upon complexation, the polarity of the metal is reduced due to the partial sharing of positive charges with donor groups and possible electron delocalization over the chelate ring [10]. This leads to stable complexes with improved properties compared to the individual components [10]. Consequently, The ability of dithiocarbamate ligands to coordinate with metals imparts unique chemical and biological properties to the resulting complex. These complexes have been explored for their antioxidant, cytotoxic, and anti-inflammatory activities [10]. As antioxidants, dithiocarbamate complexes exhibit the capacity to scavenge free radicals and protect cells from oxidative stress, even though the mechanistic principle of operation is not very clear[10, 11]. Furthermore, dithiocarbamate complexes have demonstrated cytotoxic properties against different cancer cell lines, with their mechanism of cytotoxicity thought to involve various pathways, including the generation of reactive oxygen species (ROS), interference with cellular signalling, and induction of apoptosis [10, 12]. The ability of dithiocarbamate complexes to interact with critical biomolecules, such as proteins and enzymes, has been thought to also contribute to their cytotoxic effects [10]. In addition, dithiocarbamate complexes have shown promising anti-inflammatory properties, as indicated in other literature reports [8]. Dithiocarbamate compounds have been implicated in the modulation of inflammation by inhibiting the expression of pro-inflammatory cytokines, such as interleukin-6 (IL-6) and tumor necrosis factor-alpha (TNF-α) [13]. These compounds can interfere with the signalling pathways involved in inflammation, providing potential therapeutic options for inflammatory conditions.

In the context of biological applications, Lewis base adducts of dithiocarbamate complexes exhibit unique chemical and biological properties. These adducts often involve the coordination of Lewis bases with bidentate *N, N*-donor bases such as 2,2'-bipyridine, 1,10-phenanthroline, pyridine, methyl pyridine, and triphenylphosphine[14]. The formation of Lewis base adducts can alter the reactivity, stability, and biological activity of dithiocarbamate complexes, leading to enhanced performance in various applications [15, 16]. One key aspect of the biological usefulness of Lewis base adducts is their impact on metal coordination. The coordination of Lewis bases increases the coordination number of the metal center, enabling the formation of more stable complexes with improved properties [9]. This enhanced stability can contribute to improved biological activity and bioavailability of the dithiocarbamate complexes [9]. Additionally, Lewis base adducts of dithiocarbamate complexes can exhibit altered chemical reactivity, which can be advantageous for biological applications[14]. The presence of Lewis bases can modulate the redox properties and electron-transfer reactions of the complexes, influencing their interactions with biological targets and cellular processes [14]. Furthermore, incorporating Lewis bases in dithiocarbamate complexes can provide specific functional groups or binding

motifs that enhance the interaction with biological targets. This can result in improved selectivity and affinity towards specific biological receptors or enzymes, enabling targeted therapeutic interventions [9, 14, 16].

In this current study, therefore, and in continuation of our research on Ni and Zn(II) adducts, we herein report the cytotoxicity, antioxidant, and anti-inflammatory activities of some new bathophenathroline adducts of Ni(II) and Zn(II) of *N*-methyl or ethyl-*N*-phenyldithiocarbamate. The most probable structural geometry of the synthesized adducts was characterized using various spectroscopy techniques. The antioxidant properties were ascertained using four commonly used assays, while the cytotoxicity and anti-inflammatory studies were carried out using MTT and bovine serum assays, respectively.

2 Experimental

2.1 Materials and Methods

The chemicals used in this study were commercially purchased and used as received without any further purification. Zinc(II) acetate, nickel(II) chloride, and bathophenathroline (4,7-Diphenyl-1,10-phenanthroline) (L^3) were provided by Merck/Sigma-Aldrich. The melting points of the adducts were determined using Stuart SMP10 melting point apparatus. Elemental analysis (CHNS) was recorded using the Costech ECS 4010 elemental analyzer, while infrared spectra were captured using an FTIR spectrometer (Alpha Bruker, frequency range 4000–400 cm^{-1}). Nuclear magnetic resonance (^1H and ^{13}C) spectra were obtained using a Bruker Avance III 600 MHz NMR spectrometer with $CDCL_3$ as the solvent and tetramethylsilane as an internal standard. The multiplicities of the signals in the ^1H NMR were given with chemical shifts, where s represents singlet, d represents doublet, t represents triplet, q represents quartet, and m represents multiplet.

2.2 Preparation of Bathophenanthroline Adducts of Ni(II) and Zn(II) $[M(L)_2L^3]$.

The formation of Ni(II) and Zn(II) of *N*-methyl or ethyl-*N*-phenyl dithiocarbamate precursor complexes $\mathbf{[M(L)_2]}$ followed a previously published methodology with slight modifications as reported by our group [17]. To obtain high-quality samples for the synthesis of each corresponding adduct, the precursor complexes subsequently recrystallized in chloroform with slow evaporation. To form the adducts $\mathbf{[M(L)_2L^3]}$ of respective Zn(II) and Ni(II) complexes, 20 mL of the hot mixture of chloroform of bathophenanthroline of (0.02 mol, 0.10 g) was added into the hot 25 mL aqueous mixture of synthesized precursor complexes $[M(L)_2]$ of (0.02 mol, 0.05 g) (Where L= (L^1 methyl) and (L^2 ethyl); BTP= bathophenanthroline). The resulting yellowish (Zn) or green (Ni) mixture was refluxed for 3 h and then was cooled, filtered, and allowed to evaporate gently under vacuum [18]. After 48 h, the produced deep-green or light-yellow or solid extract was obtained. The respective adducts are represented as $[Zn(L^1)_2L^3]$, $[Zn(L^2)_2L^3]$, $[Ni(L^1)_2L^3]$, $[Ni(L^2)_2L^3]$, respectively, where (L^1 = methyl, L^2 = ethyl, L^3 = bathophenanthroline). The obtained result of the characterizations of the adducts is presented in Tables 1, 2, 3.

2.3 Free Radical Scavenging Activity Using 2,2-diphenyl-1picrylhdrazyl (DPPH) Assay

Using an automatic pipette, 150 mL of each sample and ascorbic acid (AA) were put into the first row of 96 well plates (containing 150 mL of ethanol). 150 mL of the solution were pipetted into the second well and then to the other wells, to serially dilute to from 50 to 1.56 solution. A DPPH (0.15 mM; 250 µL) solution was added to each well containing samples, and the plates were left in the dark for 30 minutes. The blank solely included DMSO and DPPH solution. A microplate reader (680-BIORAD, USA) was used to detect absorbance at 517 nm. The % antioxidant activity was calculated using Eq. 1). The percentage inhibition, which reflects the scavenging activities was calculated using Eq. 1)

$$(\%)\text{inhibition} = \frac{[Ab - As]}{Ab} \times 100 \quad (1)$$

Ab = absorbance of control; As = absorbance of adduct or AA.

The 50% inhibition concentration (IC_{50}) were calculated using the plot of the % inhibition to concentration.

Table 1 Selected relevant FT-IR peaks for the prepared adducts

Sample Codes	Aromatic-CH	Aliphatic-CH_3	C=N	C_2–N	C=S	Zn-S	Zn-N
$[Zn(L^1)_2L^3]$	3044	2929	1426	1244	972	622	546
$[Zn(L^2)_2L^3]$	3042	2921	1489	1264	1003	619	551
$[Ni(L^1)_2L^3]$	3037	2922	1431	1259	970	623	544
$[Ni(L^2)_2L^3]$	3016	2924	1368	1218	989	622	540

Table 2 Data collected for the percentage yield, melting points, and the elemental analysis for the prepared adducts

Sample Codes	Yield / Mt. Point (°C)	Mol. Formula	Mol. Mass ($gmol^{-1}$)	C (%)		H (%)		N (%)		S (%)	
				Calculated	Found	Calculated	Found	Calculated	Found	Calculated	Found
$[Zn(L^1)_2L^3]$	0.32 g (88%) 186–188	$C_{40}H_{34}N_4S_4Zn$	764.36	62.85	62.83	4.48	4.47	7.33	7.34	16.78	16.80
$[Zn(L^2)_2L^3]$	0.28 g (83%) 199–201	$C_{42}H_{40}N_4S_4Zn$	794.43	63.50	63.52	5.08	5.09	7.05	7.03	16.14	16.15
$[Ni(L^1)_2L^3]$	0.31 g (85%) 197–199	$C_{40}H_{36}N_4S_4Ni$	759.69	63.24	63.22	4.78	4.79	7.73	7.75	16.88	16.90.
$Ni(L^2)_2L^3]$	0.22 g (64%) 207–209	$C_{42}H_{40}N_4S_4Ni$	787.75	64.04	64.06	5.12	5.13	7.11	7.13	16.28	16.26

2.4 Nitric Oxide (NO) Assay

The method used to investigate nitric oxide scavenging followed a previously reported approach [19]. sodium nitroprusside (2 mL, 10 mM) were mixed with respective adducts in phosphate-buffered saline (0.5 mM; pH 7.4; at 25 °C for 4 hr). Afterward, the adducts' solution or standard AA of about 0.5 mL was mixed with Griess reagent (at 25 °C for 30 min). These mixed solutions were pipetted and their absorbance was measured in a 96-well microplate, at an absorption wavelength of 540 nm. This experiment were performed three time for each adduct and AA. The % scavenging properties were then estimated using Eq. (2).

$$\%\text{scavenged[NO]} = \frac{[\text{Ab} - \text{As}]}{\text{Ab}} \times 100 \tag{2}$$

Ab = absorbance of the blank; As = absorbance of the adducts or AA. The 50% inhibition concentration (IC_{50}) were calculated using the plot of the % inhibition to concentration.

2.5 Hydrogen Peroxide (HP) Assay

Following a previous approach reported in literature, the hydrogen peroxide scavenging potentials were investigated [20]. About 5 mL of adducts or AA, dissolved in 1% and serially diluted from 50 to 1.56 µM were mixed with 0.5 mL of H_2O_2 solution prepared in a phosphate buffer (0.1 M: pH 7.4) and incubated at 25 °C for 10 minutes. Using an automatic pipette these prepared samples were (250 µL) transferred into a 96-well microplate, and the absorbance at 405 nm was measured. The adduct % scavenging properties were then calculated (see Eq. 3).

$$\%\ \text{scavenged}\left[H_2O_2\right] = \frac{[\text{Ab} - \text{As}]}{\text{Ab}} \times 100 \tag{3}$$

Ab = absorbance of the blank; As = absorbance of the adduct or AA

2.6 Reducing Power Assay (Ferric Reducing Power)

The methodology followed the reported approach by Oyaizu [21]. Approximately 0.3 mL of various adducts or AA concentrations of were added to an equal amount of potassium ferricyanide and phosphate buffer. This mixed samples were shaken vigorously using a sonicator followed by incubation at 50 °C. On bringing the resulting mixture to 25 °C, 0.2 mL of 10% trichloroacetic acid was added and centrifuged at 4500 rpm for 15 min. From this

Table 3 Chemical shift obtained from the Proton and Carbon NMR spectra for the prepared adducts

Sample codes	N-$C_6\underline{H}_5$	N-$C\underline{H}_3$	N-$C_2\underline{H}_5$	BP
$[Zn(L^1)_2(BP)]$	7.31–7.22 (m,10H)	3.78 (s, 6H)	–	9.65(d), 7.99(s) 7.49(t), (m, 6H) 7.56(-($C6H_5)_2$) (m)
$[Zn(L^2)_2(BP)]$	7.44–7.25 (m, 10H)	–	4.21 (q, 4H) 1.29 (t, 6H)	8.82(d), 7.58(s) 7.43(t), (m, 6H) 7.37(-($C_6H_5)_2$) (m)

Sample codes	-$C\underline{S}_2$	N-$C_6\underline{H}_5$	N-$C\underline{H}_3$	N-$C_2\underline{H}_5$	BP
$[Zn(L^1)_2(BP)]$	210.47	148.31–124.31	47.18	–	148.55–125.72
$[Zn(L^2)_2(BP)]$	210.47	146.37–127.43	–	64.78 ($C\underline{H}_2$) 12.84 ($C\underline{H}_3$)	149.87–122.0

mixture, 100 µL was taken and mixed with ferric chloride (20 µL) and distilled water (100 µL). The absorbance was measured at 700 nm after pipetting into a 96-well microplate. This was repeated thrice.

2.7 Cytotoxicity Activity of the Adduct Using MTT Assay

The assay is based on the reduction of a yellow tetrazolium salt (3- (4,5-dimethylthiazol-2-yl)-2,5-diphenyltetrazolium bromide or MTT) to purple formazan crystals by metabolically active cells. The procedure followed a previously reported approach with slight modifications [22]. The toxicity of adducts was screened against human cervical cancer (HeLa) and embryonic kidney 293 (HEK 293) cell lines. Both cell lines were cultured overnight at 37 °C in 25 cm^2 tissue culture flasks in EMEM with 10% fetal bovine serum (FBS) and 1% Penicillin-Streptomycin. The cells were then seeded in 96-well plates at a density of 1 × 105 cells/mL and incubated with the adduct samples at varying concentrations between 25 to 150 g/mL with a standard of 5-Fluorouracil. Positive control with untreated cells was included. The acquired cells were cultured for 24–48 h before being used for the test. To carry out the MTT assay, the media was changed with a new medium (10% MTT reagent; 5 mg/mL in PBS) and incubated (for 4 h at 37 °C) and the formazan crystals dissolved in 100 µL of DMSO. These absorbance of the mixtures were then measured at 570 nm using DMSO as the blank in a microplate reader. The tests were repeated three times and the percentage of viability of the cells were estimated as seen in Eq.4:

$$(\%)\text{Inhibition} = \frac{\text{Mean value of test compound}}{\text{Mean value of unreacted}} \times 100 \quad (4)$$

2.8 Anti-inflammatory Activity Study Using Egg Albumin Denaturation Assay.

The albumin denaturation assay is commonly used to evaluate the anti-inflammatory properties of various substances. The approach followed an already-reported methodology in literature with slight modifications [23]. A solution mixture of 2.8 mL of phosphate-buffered saline solution (pH 6.4), 0.2 mL of egg albumin, and about 2 mL of either the adduct or standard drug is made. This is followed by the incubation of the mixture for 20 min at 37°C and then boiling in a water bath for 10 minutes at 70 °C. Next, 250 µL of the resultant mixture is dispensed into a 96-well microplate where the absorbance is measured at 655 nm using a microplate reader (AMR-100 China). A standard anti-inflammatory drug like diclofenac is commonly used to compare the activity. The % protein denaturation inhibition of the adduct and diclofenac is estimated formular (5)

$$\%\text{Inhibition} = \left[\frac{\text{Vt}}{\text{Vc}} - 1\right] \times 100 \quad (5)$$

Where Vt = absorbance of adduct and diclofenac; Vc = absorbance of the control.

3 Results and Discussion

3.1 Synthesis

The synthesis of the respective parent complexes of both Zn and Ni are already reported in literature, which proceeds by replacing the corresponding chloride/acetate ions in the used metal salts with dithiocarbamate ligands. Subsequently, the bathophenanthroline adduct of these complexes was obtained by reacting the phenanthroline

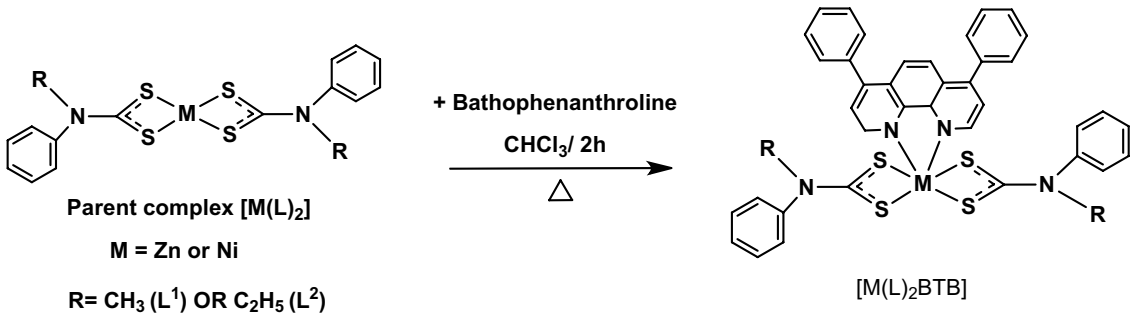

Sch. 1 Synthesis scheme of phenanthroline adducts of N–alkyl–N–phenyldithiocarbamate complexes

base with the respective precursor parent complexes, as depicted in the Sch. 1. Generally, the prepared adducts exhibited a green and yellow colour for the Ni and Zn adducts, respectively. These adducts were slightly soluble in soluble in dichloromethane, chloroform, alcohols, and dimethyl sulfoxide. However, they are insoluble in n-hexane.

3.2 Infrared Spectroscopic Studies of the Prepared of Zn and Ni Adducts.

Previous studies have established the important and relevant infrared peaks for different dithiocarbonate complexes and their adducts[24, 25]. These were then examined and compared with literature[26]. In all the adducts, the stretching vibration in the range of 1489 – 1426 cm^{-1} associated with the (C = N) bond was observed. This vibration is observed at a lower frequency compared to the parent complexes, which exhibit stretching vibrations between 1490 and 1454 cm^{-1}. The decrease in wavelength for the (C–N) bond in adducts is attributed to electron migration from the N atom of pyridine moiety, resulting in increased electron density of the thioureide group [27]. Additionally, the strong single peak found in the region between 1003 and 970 cm^{-1} represents the stretching υ(C–S) vibrational frequency for a symmetrically bonded dithiocarbamate ligand to a metal center [28]. The appearance of a strong single unsplit peak in this region suggests bidentate coordination between the ligand and the metal center [29]. Other important stretching bands, including the υ(C–H) of an SP^2 hybridized carbon, were observed in the region between around 3015–3044 cm^{-1} in all the prepared phenanthroline adducts [27]. According to previous reports, bands associated with the pyridine moiety in the adducts appeared around 1601–1605 cm^{-1}, although some were concealed by the dithiocarbamate moiety [30]. Moreover, the appearance of a band between 546–540 cm^{-1}, absent in the parent complexes, indicates the stretching vibration of υ(M–N), originating from the bond between the metal and the Lewis bases [31].

3.3 NMR Spectroscopic Studies of the Prepared Zn and Ni Adducts.

Chemical shifts obtained from the NMR (^1H and ^{13}C) characterization of the adduct complexes have been abstracted and presented in Table 1. However, the NMR characterization of the Ni parent complexes **[Ni(L)$_2$]** for both L^1 and L^2 was not carried out due to the paramagnetic nature, resulting from the four coordination around the Ni metal center, which confers a planar geometry. Nevertheless, proton signals from each adduct derived from L^1 and L^2 for the Zn counterparts have been abstracted and systematically presented in Table 1. Hence, for the adduct complexes derived from *N*-methyl-*N*-phenyldithiocarbamate (L^1), the proton signals found between 3.78 ppm were assigned to the protons of the *N*-methyl group [32]. Similarly, the proton signals of the methylene and methyl groups from the *N*-ethyl-*N*-phenyldithiocarbamate (L^2) moiety were found to resonate as quadruplets and triplets at 4.21 and 1.29 ppm, respectively [24], which are somewhat lower than the in the parent complex (N–CH_2 = 4.24 ppm; –CH_3 = 1.32 ppm). Also, the proton signals of the aromatic rings from the *N*-phenyl groups were found between 7.44 and 7.22 ppm for both ligand derivatives (that is, L^1 and L^2), the region in which these shifts occurred was also slightly lower than in the parent complex (N–C_6H_5 = 7.27–7.48 ppm). These observed chemical shifts are consistent with literature[32, 33]. Generally, the observed marginally low shifts in the Zn(II) adducts have consequently been thought to emerge due to the reduction in the deshielding effect of the electronegative N-atom as the distance between the nitrogen and the carbon bearing the protons increases[34]. Furthermore, other multiplet signals attributed to protons of the aromatic rings bearing the N of the 1, 10 phenanthroline moieties occurred downfield in the region between 9.65 and 7.42 ppm [35–37].

For the obtained ^{13}C NMR spectra, the weak peak of the thioureide carbon bond in the adducts appeared at 210.47 ppm in both spectra of the adduct derivatives. The presence of attached phenanthroline derivatives caused additional deshielding effects, resulting in a shift of

approximately 4 ppm compared to that observed in parent complexes (206.47 ppm). The electron density displacement from carbon to nitrogen in the adduct complexes was attributed to the bonding of the Lewis base to the metal atom. This bonding initiation led to a reduction in the partial double bond character of the C=N bond, as supported by the FTIR spectra [38, 39]. Additionally, for the parent complex moiety in the adduct, two strong carbon signals ascribed to the carbon of methylene (N–CH_2–) and methyl (–CH_3–) group of L^2 moiety resonated at 64.78 and 12.84 ppm, while a single strong methyl carbon signal of L^2 moiety resonated at 47.18, which is consistent with other reports [40–42]. In the adducts, other carbon signals in both L^1 and L^2, within the range of 148.31 – 124.31 ppm, can be attributed to the phenyl carbon group (N–C_6H_5) of both the *N*-methyl and *N*-ethyl fragments. Moreover, the aromatic carbons of the phenanthroline moieties exhibited resonances between 149.87 and 122.01 ppm, similar to other previous studies [9]. A representative proton and carbon spectra of **[Zn(L^1)$_2$L^3]** are presented in Figure 1.

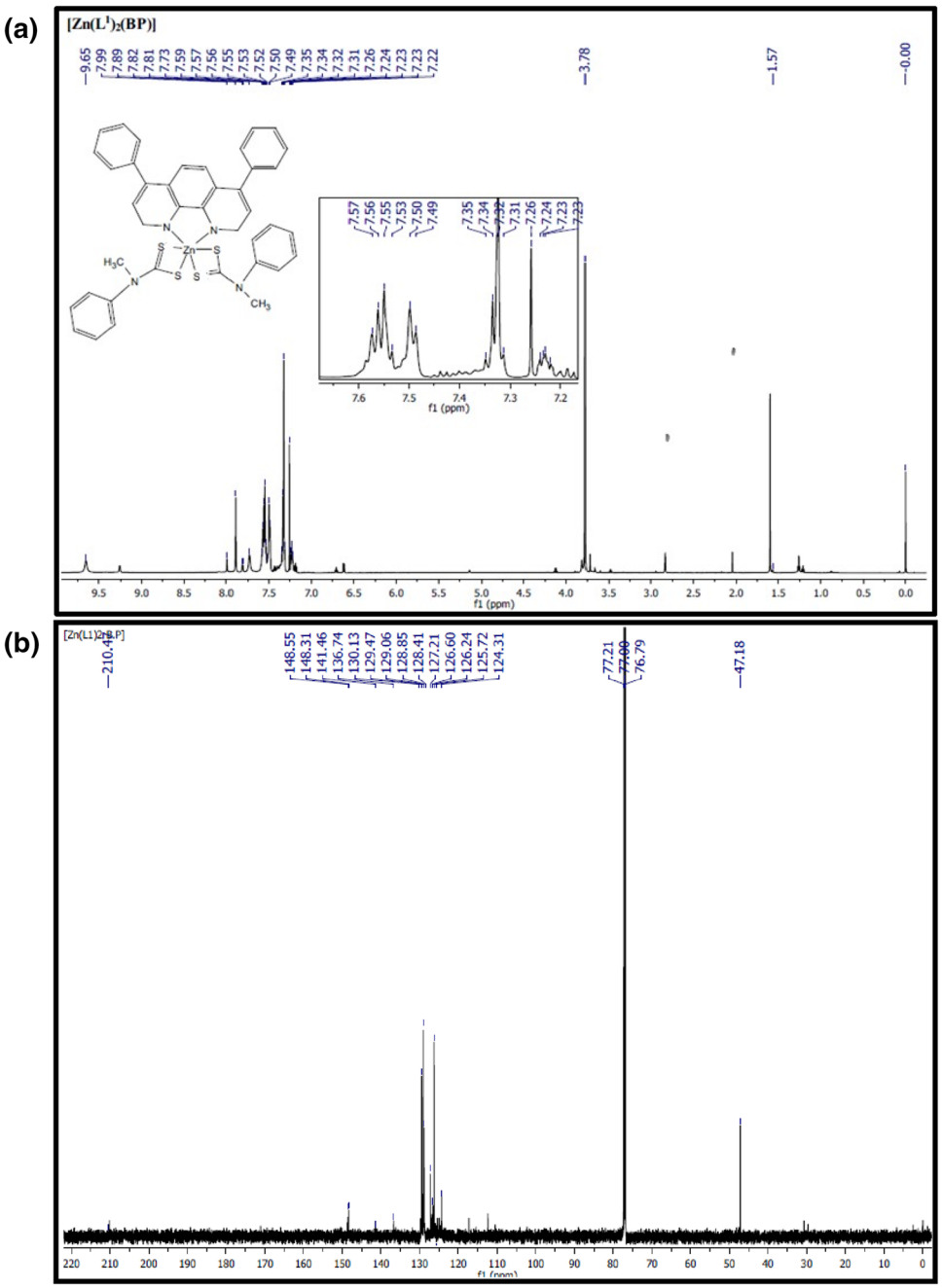

Fig. 1 1H (**a**) and 13C (**b**) spectra of adducts Zn (II) N-alkyl-N-phenyldithiocarbamate complexes **[M(L1)2L3]**

3.4 Antioxidant Property Evaluation of the Prepared Zn(II) and Ni(II) Adducts

All the assays used in this study, namely DPPH (2,2-diphenyl-1-picrylhydrazyl), Nitric Oxide, Hydrogen Peroxide, and Reducing power assay, are notable and well-documented assays commonly used to evaluate the antioxidant activity of compounds or samples [43]. The DPPH measures the ability of an antioxidant to scavenge or neutralize the DPPH radical, indicating its free radical scavenging capacity [44]. A higher percentage of DPPH radical scavenging indicates stronger antioxidant activity [44]. Nitric Oxide assay measures the ability of an antioxidant to inhibit the production of NO, reflecting its potential to mitigate oxidative stress and protect against related damage [45]. Seeing that this free radical is involved in various physiological processes, the need to remove this radical stem when it is overly accumulated in the body leads to oxidative stress and tissue damage [45]. Also, the Hydrogen Peroxide assay evaluates the ability of an antioxidant to break down or neutralize hydrogen peroxide [46]. The higher the antioxidant activity, the more effectively it can reduce hydrogen peroxide levels, indicating its potential protective effects against oxidative stress [46]. Additionally, reducing power assay measures the capacity of an antioxidant to convert oxidized substances into their reduced forms. A higher reducing power indicates stronger antioxidant activity, reflecting the ability to neutralize and stabilize free radicals or reactive species [43].

Generally, these assays provide valuable information about the antioxidant potential of compounds or samples by evaluating their ability to scavenge free radicals, inhibit oxidative stress, reduce reactive species, and maintain cellular redox balance. They are essential tools in assessing the effectiveness of antioxidants in various applications, such as pharmaceuticals, functional foods, and natural product research [43]. In this study, therefore, the half maximal inhibitory concentration (IC_{50}) of each assay in comparison to a known commonly used antioxidant (ascorbic acid) was estimated using standard literature procedure and summarily presented in Table 4. This IC_{50} value is determined by generating a dose-response curve and analyzing the relationship between the concentration of the inhibitory substance and the corresponding biological response. Thus,

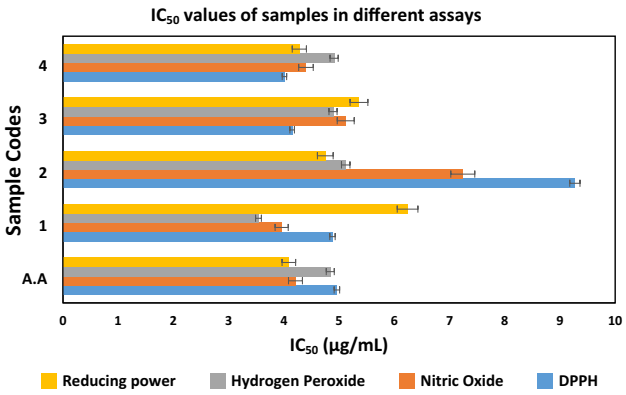

Fig. 2 The histogram plot of the estimated IC50 values of adducts and ascorbic acid in different antioxidant assays

the concentration required to inhibit 50% of the maximum response is identified as the IC_{50} value. The collected data in Table 4 has been plotted as a histogram in Fig. 2. From this table and figure, the adducts had IC_{50} values in the following ranges 4.01–9.27, 3.96–7.24, 3.54–5.12 and 4.28–6.24 µg/mL in the DPPH, Nitric oxide, hydrogen peroxide and reducing power assays, respectively. Specifically, the adducts had the best response comparable to ascorbic acid in the DPPH assay, except for sample $\mathbf{[Zn(L^2)_2L^3]}$ (9.27 ± 0.03 µg/mL), which is twice less than the estimated value for ascorbic acid (4.96 ± 0.01 µg/mL). Nevertheless, in this assay, sample $\mathbf{[Ni(L^2)_2L^3]}$ possessed the best activity, about 0.95 µg/mL better than the ascorbic acid. Similarly, in both Nitric oxide and Peroxide assays, the estimated IC_{50} values showed that $\mathbf{[Zn(L^2)_2L^3]}$ (**NO** = 7.24 ± 0.04; **HP** = 5.12 ± 0.04 µg/mL) possessed the weakest scavenging activity in comparison to ascorbic acid (**NO** = 4.21 ± 0.03; **HP** = 4.84 ± 0.02 µg/mL) in both assays. However, in both assays, $[Zn(L^1)_2L^3]$ (NO = 3.96 ± 0.02; HP = 3.54 ± 0.01 µg/mL) possessed the best activity, which is better than the standard ascorbic acid. Additionally, in the reducing power assay, none of the adducts had better activity than the standard ascorbic acid, as indicated in the plot. However, amongst the adduct, $\mathbf{[Ni(L^2)_2L^3]}$ (4.28 ± 0.03 µg/mL) and $\mathbf{[Zn(L^1)_2L^3]}$ (6.24 ± 0.04 µg/mL) possessed the best and the weakest activity in comparison to ascorbic acid (4.09 ± 0.08µg/mL). Therefore, the obtained result showed no noticeable trend in activity

Table 4 The half maximal inhibitory concentration (IC_{50}) values in µg/mL of adducts and ascorbic acid in different antioxidant assays

No	Samples name	DPPH	Nitric oxide (NO)	Hydrogen peroxide (HP)	Reducing power (RP)
A.A	Ascorbic acid	4.96± 0.01	4.21 ±0.03	4.84 ± 0.02	4.09 ± 0.08
1	$[Zn(L^1)_2L^3]$	4.88±0.05	3.96±0.02	3.54±0.01	6.24±0.04
2	$[Zn(L^2)_2L^3]$	9.27±0.03	7.24±0.04	5.12±0.04	4.75±0.04
3	$[Ni(L^1)_2L^3]$	4.15±0.03	5.12±0.02	4.89±0.02	5.36±0.03
4	$[Ni(L^2)_2L^3]$	4.01±0.04	4.40±0.04	4.91±0.04	4.28±0.03

patterns based on their structural relationship, even though similar parent dithiocarbamate complexes and Lewis bases were used. Nevertheless, generally in all the assays, the best performing free radical scavenging adduct (antioxidant agent), with a broad-spectrum potential, in this study seems to be between **[Zn(L^1)$_2$L^3]** and **[Ni(L^2)$_2$L^3]** upon comparing to ascorbic acid**.**

3.5 Cytotoxicity of the Phenanthroline Adducts of Zn(II) and Ni(II) N-alkyl-N-phenyldithiocarbamate [M(L)$_2$L^3]

The MTT (3-[4,5-dimethylthiazol-2-yl]-2,5 diphenyl tetrazolium bromide) assay is a commonly used approach to assess cytotoxicity and measure cell viability [47]. This assay is based on the conversion of MTT into formazan crystals by living cells, which is directly proportional to mitochondrial activity and serves as an indicator of cell viability [47]. The fundamental principle of the MTT assay is based on the observation that the mitochondrial activity of most viable cells remains constant. Consequently, any increase or decrease in the number of viable cells is directly proportional to mitochondrial activity. This principle is exploited by measuring the conversion of the tetrazolium salt MTT into formazan crystals, reflecting the mitochondrial activity of the cells. The resulting formazan crystals can be solubilized, enabling homogeneous measurement. The detection of changes in viable cell number is accomplished by quantifying formazan concentration, typically through optical density (OD) measurements at 540 and 720 nm using a plate reader. In the context of drug sensitivity measurements, the MTT assay compares the OD values of wells containing cells incubated with drugs to those without drug exposure. This comparison allows for the evaluation of the impact of drugs on cell viability. The MTT assay is applicable for assessing drug sensitivity in both established cell lines and primary cells. In the case of dividing cells, such as cell lines, the decrease in cell number reflects inhibition of cell growth. The drug sensitivity is typically quantified as the concentration of the drug required to achieve 50% growth inhibition compared to the growth of untreated control cells. This concentration is referred to as the 50% inhibitory concentration (IC_{50}) [47]. Hence, in our study, two cell lines of human cervical cancer (HeLa) and embryonic kidney 293 (HEK 293) were employed to screen the cytotoxicity of the prepared adduct, and a dose-dependent profile was observed at the used concentration range of 10–100 μgmL^{-1}. The degree of activity in percentages and the estimated 50% growth inhibition concentration (IC_{50}) of the adducts and the 5-Flurouracil (5 FU), a standard drug, is thus presented summarily as Table 5. In the HeLa cell line, at 10 μgmL^{-1}, **[Zn(L^2)$_2$L^3]** showed the lowest cell viability of about 12.98 %, which is far superior to the value estimated for 5-Flurouracil (45.40%). In comparison **[Ni(L^1)$_2$L^3]** showed the highest cell viability of about 95.75% at the same concentration. Whereas, at the used highest concentration of 100 μgmL^{-1}, in the same cell line, **[Ni(L^2)$_2$L^3]** possessed about 11.98% cell viability, which is slightly less than the value estimated for 5-Flurouracil (11.98 %), while the least cell viability percentage was found for **[Ni(L^1)$_2$L^3]** at the same concentration. Nevertheless, the IC_{50} value for both **[Zn(L^1)$_2$L^3]** and **[Ni(L^2)$_2$L^3]** were estimated to be 0.011 and 14.76 µM, respectively. These are better than the estimated IC_{50} value of the standard 5-Flurouracil (17.48 µM).

Table 5 The percentage (%) cell viability of human cervical cancer (HeLa) and embryonic kidney 293 (HEK 293) against different concentrations of the phenanthroline adducts of Zn(II) and Ni(II) N-alkyl-N-phenyldithiocarbamate **[M(L)$_2$L^3]**

	Samples in HeLa	10 μgmL^{-1}	25 μgmL^{-1}	50 μgmL^{-1}	100 μgmL^{-1}	$IC_{50}\mu M$
Control-1	Cells only	100 ± 0.01	100 ± 0.01	100 ± 0.01	100 ± 0.01	–
Control-2	Cell + 10 µl DMSO	84 ± 0.02	84 ± 0.02	84 ± 0.02	84 ± 0.02	–
5 FU	5-Fluorouracil	76,99 ± 0.03	51,33 ± 0.04	35,07 ± 0.02	11.12 ± 0.02	17.48
1	[Zn(L^1)$_2$L^3]	20 ± 4.64	25.56 ± 12.72	10.71 ± 6.456	14.13 ± 10.23	0.011
2	[Zn(L^2)$_2$L^3]	12.98 ± 2.59	6.66 ± 4.62	14.64 ± 6.36	16.89 ± 8.82	n/a
3	[Ni(L^1)$_2$L^3]	95.75 ± 0.03	71.46 ± 0.04	47.19 ± 0.04	36.33 ± 0.03	53.75
4	[Ni(L^2)$_2$L^3]	58.57 ± 0.03	39.55 ± 0.02	22.10 ± 0.03	11.98 ± 0.01	14.76
	Samples in HEK293	10 μgmL^{-1}	25 μgmL^{-1}	50 μgmL^{-1}	100 μgmL^{-1}	$IC_{50}\mu M$
Control-1	Cells only	100±0.05	100±0.05	100±0.05	100±0.05	-
Control-2	Cell + 10µl DMSO	100±0.127	100±0.127	100±0.127	100±0.127	-
5 FU	5-Fluorouracil	45.40±0.04	51.91±0.003	35.40±0.01	11.33±0.01	6.05
1	[Zn(L^1)$_2$L^3]	28.10±4.68	17.92±11.19	22.44±22.32	28.15±17.20	n/a
2	[Zn(L^2)$_2$L^3]	49.76±6.86	40.87±8.15	33.94±13.41	30.71±11.49	8.91
3	[Ni(L^1)$_2$L^3]	60.49±0.06	47.09±0.03	18.92±0.01	4.27±0.011	17.02
4	[Ni(L^2)$_2$L^3]	76.13±0.05	66.72±0.04	47.41±0.03	16.92±0.03	35.89

Specifically, **[Zn(L^1)$_2$L^3]** possessed a cytotoxicity approximately 159 times superior to standard 5-Flurouracil. **[Zn(L^2)$_2$L^3]**, on the other hand, possessed a cytotoxicity that is well above 500 µM, which is outside of a usable range compared to the standard drug.

Although this activity cytotoxicity of some of the adducts is very outstanding, it is important to compare the cytotoxicity of a probable drug material in both cancer and normal human cell lines to allow for the assessment of selectivity, understanding the response of normal cells, evaluating the safety, and predicting clinical relevance. This approach provides valuable information for developing and optimizing potential cancer treatments. Therefore, HEK 293, an immortalized cell line, was used to understand the selectivity towards the used HeLa cancer cell line. This implies, in this case, that the higher the % cell viability in comparison to the standard drug, the better the adduct. At the lowest used concentration, **[Ni(L^2)$_2$L^3]**, with a percentage viability of about 76.13%, possessed the best activity, while **[Zn(L^1)$_2$L^3]**, with about 28.10%, possessed the weakest desirable activity. In the used highest concentration, from the observed data in the table, **[Zn(L^2)$_2$L^3]** possessed the best-desired activity, while [Ni(L^1)$_2$L^3] possessed the least desirable activity based on the cell survival %. Consequently, in terms of IC_{50}, the best activity exhibited by any of the adducts was observed for **[Zn(L^1)$_2$L^3]**, which was out of range in the HEK 293 cell line in comparison to the standard, which possessed an IC_{50} value of 6.05 µM. The least activity was observed for **[Ni(L^2)$_2$L^3]**. Furthermore, in both cell lines, the most useful activity, due to selectivity towards the cancer cell line, is **[Zn(L^1)$_2$L^3],** while the least performing adduct in the used cell lines is **[Zn(L^2)$_2$L^3],** seeing that it does not have any useful activity in the HeLa cancer cell line and yet cytotoxic towards an ordinary, normal cell line. Therefore, generally, the observed cytotoxic activities of most of the adducts, according to other literature reports, may have emerged from the increased lipophilicity brought about by the presence of the phenyl groups on the -NCS_2 backbone and more than one heterocyclic bipyridine ring found within their structure[48].

3.6 Anti-inflammatory Study

As already indicated in literature, it is desirable for all anticancer agents to exhibit anti-inflammatory effects [49]. Despite several research efforts over the years, which have led to the discovery of many medicinal agents, acute and chronic inflammatory diseases still pose significant health concerns worldwide, albeit with certain acute side effects [50]. Therefore, there is an ongoing need to develop novel anti-inflammatory agents with minimal or no side effects. Considering the interconnectedness of anticancer and anti-inflammatory properties. The denaturation assay method used in this study works based on the principle of subjecting egg albumin to different conditions, such as varying concentrations, to observe its denaturation. The prevention or inhibition of protein denaturation is considered beneficial, as protein denaturation is thought to contribute to inflammation. In this study, the collected data showing the estimated minimum inhibitory concentration for the anti-inflammatory activities of both adducts and standard diclofenac drug is presented Table 6 presents. All the adducts showed a good to moderate anti-inflammatory activity according to the estimated IC_{50} compared to the standard diclofenac. Specifically, the prepared adduct **[Zn(L^2)$_2$L^3]** with an IC_{50} value of 2.90 ± 0.01 µM showed better activity than the diclofenac 2.94 ± 0.01 µM. Both **[Zn(L^1)$_2$L^3]** and **[Ni(L^2)$_2$L^3]** possessed similar activity in this assay, while **[Ni(L^2)$_2$L^3]** had the weakest activity in the group but showed a moderate anti-inflammatory properties in comparison to the standard drug.

Table 6 Estimated minimum inhibitory concentration for the anti-inflammatory activities of both adducts and diclofenac

No	Samples name	Anti-inflammation (IC_{50} µM)
1	[Zn(L^1)$_2$L^3]	3.21±0.01
2	[Zn(L^2)$_2$L^3]	2.90±0.01
3	[Ni(L^1)$_2$L^3]	3.21±0.02
4	[Ni(L^2)$_2$L^3]	4.43±0.02
Standard	Diclofenac	2.94±0.01

4 Conclusion

The newly synthesized and characterized adducts were derived from the Lewis bases of 1,10-phenanthroline and the parent complexes of Zn(II) and Ni(II) bis(*N*-alkyl-*N*-phenyldithiocarbamate). Analytical data obtained using spectroscopic and elemental analysis studies confirmed the structure and composition of these complexes. The coordination of the Lewis base occurred in a bidentate manner, utilizing the two available nitrogen atoms, resulting in the complexes adopting an octahedral structure around the metal centers. In the antioxidant characterization study, the adduct exhibited significant properties in various assays, particularly the DPPH assay, indicating their ability to scavenge free radicals and mitigate oxidative stress. The adducts' antioxidative effects were independent of enzymatic actions and attributed to their capacity to degrade hydrogen and lipid peroxide. Furthermore, the adducts demonstrated enhanced cytotoxicity against two cell lines of human cervical cancer (HeLa) and embryonic kidney 293 (HEK 293), with **[Zn(L^1)$_2$L^3]** having the best activity due to selectivity and superior activity than the used standard drug of 5-fluorouracil in HeLa

cancer cell line and yet non-cytotoxic towards an ordinary, normal cell line. Additionally, the adducts exhibited good to moderate anti-inflammatory properties in the used albumin test approach compared to diclofenac, a controlled drug. These findings suggest that these adducts, especially **[Zn(L^{1})$_2$L^{3}],** are promising candidates for developing anticancer agents upon further clinical trials.

Funding Open access funding provided by North-West University.

Data availability All the data are already presented in the manuscript.

References

1. Sodhi RK, Paul S (2019) Metal Complexes in Medicine: An Overview and Update from Drug Design Perspective. Cancer Therapy Oncol Int J. https://doi.org/10.19080/CTOIJ.2019.14.555883
2. Patients S, in Solid Cancer PC, Hassan BAR, Yusoff ZBM, Othman MAH, Bin S, information is available at the end of the Chapter A, Http://dx.doi.org/https://doi.org/10.5772/55358 (2012) We are IntechOpen , the world ' s leading publisher of Open Access books Built by scientists , for scientists TOP 1 %. Intech 13
3. Kostova I (2023) The Role of Complexes of Biogenic Metals in Living Organisms. Inorganics (Basel). https://doi.org/10.3390/inorganics11020056
4. Steinborn D (2004) The concept of oxidation states in metal complexes. J Chem Educ 81:1148–1154. https://doi.org/10.1021/ed081p1148
5. Larson VA, Battistella B, Ray K, Lehnert N, Nam W (2020) Iron and manganese oxo complexes, oxo wall and beyond. Nat Rev Chem 4:404–419. https://doi.org/10.1038/s41570-020-0197-9
6. Pattan SR, Pawar SB, Vetal SS, Gharate UD, Bhawar SB (2012) The scope of metal complexes in drug design - A review. Indian Drugs 49:5–12
7. Caballero AB, Salas JM, Sánchez-Moreno M (2014) Metal-Based Therapeutics for Leishmaniasis. Metal-Based Therapeutics for Leishmaniasis 1–28. https://doi.org/10.5772/57376
8. Adeyemi J, Onwudiwe D (2018) Organotin(IV) Dithiocarbamate Complexes: Chemistry and Biological Activity. Molecules 23:2571. https://doi.org/10.3390/molecules23102571
9. Saiyed TA, Adeyemi JO, Onwudiwe DC (2021) The structural chemistry of zinc(ii) and nickel(ii) dithiocarbamate complexes. Open Chem 19:974–986. https://doi.org/10.1515/chem-2021-0080
10. Adeyemi JO, Onwudiwe DC (2020) The mechanisms of action involving dithiocarbamate complexes in biological systems. Inorganica Chim Acta 511:119809. https://doi.org/10.1016/j.ica.2020.119809
11. Chioma F, Ekennia AC, Osowole AA, Okafor SN, Ibeji CU, Onwudiwe DC, Ujam OT (2018) Synthesis, characterization, in-vitro antimicrobial properties, molecular docking and DFT studies of 3-{(E)-[(4,6-dimethylpyrimidin-2-yl)imino]methyl} naphthalen-2-ol and Heteroleptic Mn(II), Co(II), Ni(II) and Zn(II) complexes. Open Chem 16:184–200. https://doi.org/10.1515/chem-2018-0020
12. Buac D, Schmitt S, Ventro G, Rani Kona F, Ping Dou Q (2012) Dithiocarbamate-based coordination compounds as potent proteasome inhibitors in human cancer cells. Mini Rev Med Chem 12:1193–1201. https://doi.org/10.2174/138955712802762040
13. Cuzzocrea S, Chatterjee PK, Mazzon E, Dugo L, Serraino I, Britti D, Mazzullo G, Caputi AP, Thiemermann C (2002) Pyrrolidine dithiocarbamate attenuates the development of acute and chronic inflammation. Br J Pharmacol 135:496–510. https://doi.org/10.1038/sj.bjp.0704463
14. Odularu AT, Ajibade PA (2019) Dithiocarbamates: Challenges, Control, and Approaches to Excellent Yield, Characterization, and Their Biological Applications. Bioinorg Chem Appl 2019:1–15. https://doi.org/10.1155/2019/8260496
15. Rani PJ, Thirumaran S, Ciattini S (2014) Synthesis, spectral and antibacterial studies on Ni(II) and Zn(II) complexes involving N -furfuryl- N -isopropyldithiocarbamate (f i prdtc) and Lewis bases: X-ray structure of [Ni(f i prdtc)(NCS)(PPh 3)]. J Sulfur Chem 35:106–116. https://doi.org/10.1080/17415993.2012.751989
16. Hassan AF (2015) Synthesis, Characterization and Biological Studies of Some New Mixed Nickel (II) Complexes Containing Dithiocarbamate and 1,10-phenanthroline Ligands. J Chem Mater Res 7:9–16
17. Halimehjani AZ, Torabi S, Amani V, Notash B, Saidi MR (2015) Synthesis and characterization of metal dithiocarbamate derivatives of 3-((pyridin-2-yl)methylamino)propanenitrile: Crystal structure of [3-((pyridin-2-yl)methylamino)propanenitrile dithiocarbamato] nickel(II). Polyhedron 102:643–648. https://doi.org/10.1016/j.poly.2015.10.058
18. Sharma M, Sharma A, Sachar R (2012) Synthesis and Characterization of the Adducts of Morpholinedithioccarbamate Complexes of Oxovanadium (IV), Nickel(II), and Copper(II) with Piperidine and Morpholine. E-J Chem 9:1929–1940. https://doi.org/10.1155/2012/689501
19. Jimoh MO, Afolayan AJ, Lewu FB (2019) Antioxidant and phytochemical activities of Amaranthus caudatus L. harvested from different soils at various growth stages. Sci Rep 9:12965. https://doi.org/10.1038/s41598-019-49276-w
20. Okeleye BI, Nongogo V, Mkwetshana NT, Ndip RN (2015) Polyphenolic content and in vitro antioxidant evaluation of the stem bark extract of peltophorum africanum sond (Fabaceae). Afr J Tradit, Complement Altern Med 12:1–8. https://doi.org/10.4314/ajtcam.v12i1.1
21. Oyaizu M (1986) Studies on products of browning reaction. Antioxidative activities of products of browning reaction prepared from glucosamine. Japn J Nutr Diet 44:307–315. https://doi.org/10.5264/eiyogakuzashi.44.307
22. Tabrizi L, McArdle P, Erxleben A, Chiniforoshan H (2015) Cytotoxicity and antimicrobial activity of triorganotin(IV) complexes of phenylcyanamide prepared by sonochemical synthesis. Inorg Chim Acta 438:94–104. https://doi.org/10.1016/j.ica.2015.09.011
23. Bhattacharya S, Chandra S, Chatterjee P, Dey P (2012) Evaluation of anti-inflammatory effects of green tea and black tea: A comparative in vitro study. J Adv Pharm Technol Res 3:136. https://doi.org/10.4103/2231-4040.97298
24. Onwudiwe DC, Nthwane YB, Ekennia AC, Hosten E (2016) Synthesis, characterization and antimicrobial properties of some mixed ligand complexes of Zn(II) dithiocarbamate with different

N-donor ligands. Inorg Chim Acta 447:134–141. https://doi.org/10.1016/j.ica.2016.03.033
25. Onwudiwe DC, Kabanda MM, Ebenso EE, Hosten E (2016) Synthesis, crystal structure, thermal and theoretical studies of bis(N-ethyl-N-phenyldithiocarbamato) Ni(II) and (N-ethyl-N-phenyldithiocarbamato) (isothiocyanato) (triphenylphosphine) Ni(II). J Chem Sci 128:1081–1093. https://doi.org/10.1007/s12039-016-1111-3
26. Jamuna Rani P, Thirumaran S, Ciattini S (2015) Synthesis and characterization of Ni(II) and Zn(II) complexes of (furan-2-yl) methyl(2-(thiophen-2-yl)ethyl)dithiocarbamate (ftpedtc): X-ray structures of [Zn(ftpedtc)2(py)] and [Zn(ftpedtc)Cl(1,10-phen)]. Spectrochim Acta A Mol Biomol Spectrosc 137:1164–1173. https://doi.org/10.1016/j.saa.2014.09.019
27. Onwudiwe DC, Hosten EC (2018) Synthesis, structural characterization, and thermal stability studies of heteroleptic cadmium(II) dithiocarbamate with different pyridyl groups. J Mol Struct 1152:409–421. https://doi.org/10.1016/j.molstruc.2017.09.076
28. Sharma M, Sharma A, Sachar R (2013) Preparation and Characterization of the Adducts of Bis(N, N-diethyldithiocarbamato) oxovanadium(IV) and Copper(II) with n-Propylamine and Isopropylamine. Chem Sci Trans 2:367–374. https://doi.org/10.7598/cst2013.265
29. Bonati F, Ugo R (1967) Organotin(IV) N, N-disubstituted dithiocarbamates. J Organomet Chem 10:257–268. https://doi.org/10.1016/S0022-328X(00)93085-7
30. Saiyed TA, Adeyemi JO, Saibu GM, Singh M, Oyedeji AO, Hosten EC, Onwudiwe DC (2023) Bipyridine adducts of Zn(II) and Ni(II) bis (N-methyl-N-phenyl dithiocarbamate): Synthesis, characterization, and biological applications. J Mol Struct 1274:134335. https://doi.org/10.1016/j.molstruc.2022.134335
31. Kartina D, Wahab AW, Ahmad A, Irfandi R, Raya I (2019) In vitro antibacterial and anticancer activity of Zn(II)Valinedithiocarbamate complexes. J Phys Conf Ser. https://doi.org/10.1088/1742-6596/1341/3/032042
32. Adeyemi JO, Onwudiwe DC, Ekennia AC, Uwaoma RC, Hosten EC (2018) Synthesis, characterization and antimicrobial studies of organotin(IV) complexes of N-methyl-N-phenyldithiocarbamate. Inorg Chim Acta 477:148–159. https://doi.org/10.1016/j.ica.2018.02.034
33. Adeyemi JO, Onwudiwe DC, Hosten EC (2018) Organotin(IV) complexes derived from N-ethyl-N-phenyldithiocarbamate: Synthesis, characterization and thermal studies. J Saudi Chem Soc 22:427–438. https://doi.org/10.1016/j.jscs.2017.08.004
34. Onwudiwe DC, Ajibade PA (2013) Synthesis, Characterization and Thermal Study of Phenanthroline Adducts of Zn (II) and Cd (II) Complexes of bis-N-Alkyl-N-phenyl dithiocarbamates. Asian J Chem 25:10057–10061
35. Marandi F, Moeini K, Rudbari HA (2016) Structural and spectral study of coordination of 4,4′-dimethoxy-2,2′-bipyridine toward Zn(II) and Cd(II) containing thiocyanato or azido ligands. Zeitschrift fur Naturforschung - Sect B J Chem Sci 71:959–965. https://doi.org/10.1515/znb-2016-0083
36. Maurya VK, Singh AK, Singh RP, Yadav S, Kumar K, Prakash P, Prasad LB (2019) Synthesis and evaluation of Zn(II) dithiocarbamate complexes as potential antibacterial, antibiofilm, and antitumor agents. J Coord Chem 72:3338–3358. https://doi.org/10.1080/00958972.2019.1693041
37. Marimuthu G, Ramalingam K, Rizzoli C (2010) Synthesis, spectral, thermal and BVS investigations on ZnS4N^N/N coordination environment: Single crystal X-ray structures of bis(dibenzyldithiocarbamato)(N^N)Zinc(II) complexes (N^N=1,10-phenanthroline, tetramethylethylenediamine and 4,4′-bipyridine). Polyhedron 29:1555–1560. https://doi.org/10.1016/j.poly.2010.02.001
38. Bobinihi FF (2020) Group 10 dithiocarbamate complexes for biological applications and as single source precursors_ to metal sulphide nanoparticles. North West University, South Africa
39. Prakasam BA, Ramalingam K, Baskaran R, Bocelli G, Cantoni A (2007) Synthesis, NMR spectral and single crystal X-ray structural studies on Ni(II) dithiocarbamates with NiS2PN, NiS2PC, NiS2P2 chromophores: Crystal structures of (4-methylpiperazinecarbodithioato)(thiocyanato-N) (triphenylphosphine)nickel(II) and bis(triphen. Polyhedron 26:1133–1138. https://doi.org/10.1016/j.poly.2006.10.006
40. Onwudiwe DC, Adeyemi JO, Papane RT, Bobinihi FF, Hosten E (2021) Spectroscopic And Structural Characterization Of Zn(II) Bis(N-Ethyl-N-Ethanol Dithiocarbamate) And Its Adducts With N-Donor Ligands. J Struct Chem 62:412–421. https://doi.org/10.1134/S0022476621030070
41. Ramos-Espinosa Á, Valdés H, Teresa Ramírez-Apan M, Hernández-Ortega S, Adriana Aguilar-Castillo B, Reyes-Martínez R, Manuel Germán-Acacio J, Morales-Morales D (2017) N-(R) ethanolamine dithiocarbamate ligands and their Ni(II) and Pt(II) complexes. Evaluation of the in vitro anticancer activity of the Pt(II) derivatives. Inorg Chim Acta 466:584–590. https://doi.org/10.1016/j.ica.2017.07.035
42. Bobinihi FF, Osuntokun J, Onwudiwe DC (2018) Syntheses and characterization of nickel(II) dithiocarbamate complexes containing NiS 4 and NiS 2 PN moieties: Nickel sulphide nanoparticles from a single source precursor. J Saudi Chem Soc 22:381–395. https://doi.org/10.1016/j.jscs.2017.10.001
43. Munteanu IG, Apetrei C (2021) Analytical methods used in determining antioxidant activity: A review. Int J Mol Sci. https://doi.org/10.3390/ijms22073380
44. Blois MS (1958) Blois, M. S. (1958). Antioxidant determinations by the use of a stable free radical. Nature, 181(4617), 1199–1200. Nature 181:1199–1200
45. Marcocci L, Maguire JJ, Droy-Lefaix MT, Packer L (1994) The nitric oxide-scavenging properties of Ginkgo biloba extract EGb 761. Biochem Biophys Res Commun 201:748–755
46. Ruch RJ, Cheng S, Klaunig JE (1989) Prevention of cytotoxicity and inhibition of intercellular communication by antioxidant catechins isolated from Chinese green tea. Carcinogenesis 10:1003–1008. https://doi.org/10.1093/carcin/10.6.1003
47. van Meerloo J, Kaspers GJL, Cloos J (2011) Cell Sensitivity Assays: The MTT Assay. Cancer Cell Culture. 1:237–245
48. Knopf KM, Murphy BL, Macmillan SN, Baskin JM, Barr MP, Boros E, Wilson JJ (2017) In Vitro Anticancer Activity and in Vivo Biodistribution of Rhenium(I) Tricarbonyl Aqua Complexes. J Am Chem Soc 139:14302–14314. https://doi.org/10.1021/jacs.7b08640
49. Nath M, Vats M, Roy P (2015) Mode of action of tin-based antiproliferative agents: Biological studies of organotin(IV) derivatives of fatty acids. J Photochem Photobiol B 148:88–100. https://doi.org/10.1016/j.jphotobiol.2015.03.023
50. Saxena RS, Gupta B, Saxena KK, Singh RC, Prasad DM (1984) Study of anti-inflammatory activity in the leaves of Nyctanthes arbor tristis Linn — an Indian medicinal plant. J Ethnopharmacol 11:319–330. https://doi.org/10.1016/0378-8741(84)90077-1